Acc. Chem. Res. **2000**, *33*, 869−877

# Additive Fabrication and the Mechanisms of Nucleation and Growth in Chemical Vapor Deposition Processes

ELIZABETH L. CRANE,
GREGORY S. GIROLAMI,* AND
RALPH G. NUZZO*

*School of Chemical Sciences and Frederick Seitz Materials Research Laboratory, University of Illinois at Urbana−Champaign, Urbana, Illinois 61801*

Received February 18, 2000

**ABSTRACT**
In this Account, we present several representative studies of thin-film growth by chemical vapor deposition, with particular emphasis given to elucidating the mechanistic, energetic, and structural aspects of nucleation and growth. These understandings have allowed us to develop new methods to deposit patterned, as opposed to blanket, thin films. We show how such procedures can be exploited to effect the directed assembly (i.e., the additive fabrication) of a device architecture.

## Introduction

The growth of thin films via chemical vapor deposition (CVD) is an industrially significant process with a wide array of applications, notably in microelectronic device fabrication. In this Account we will describe aspects of the research we have undertaken to gain an understanding of CVD processes on a chemical and mechanistic level, and in so doing, we will attempt to illustrate areas of need and opportunities for research.

In general terms, chemical vapor deposition (CVD) is carried out by passing a volatized precursor (such as an organometallic or metal coordination complex) over a heated substrate.[1,2] Thermal decomposition of the precursor produces a thin-film deposit, and ideally, the ligands associated with the precursor are cleanly lost to the gas phase as reaction products.[2] Compared to other thin-film production techniques, CVD offers several significant advantages, most notably the potential for effecting selective deposition,[3−12] lower processing temperatures,[2,3,13] and enhanced conformal coverage of nonplanar substrates.[13,14] The microstructural habits of a CVD-derived film can be complex, however, and limit its utility.[1] In addition, side reactions, such as those leading to the incomplete removal of ligand-derived species, can introduce undesired impurities into the film.[15]

To better understand the causes of these undesirable features and to improve the efficiencies of CVD processes, it is useful to establish the nature and kinetics of the molecular mechanisms responsible for the decomposition of the precursor. In our research we have been especially interested in achieving selectivity in film growth and using this selectivity as a means to deposit patterned (or additive) thin-film microstructures.[16]

A CVD process usually involves several discrete mechanistic steps, most importantly those involved in nucleation and those that carry the reaction forward under steady-state conditions. In the nucleation steps, the precursor molecules generally contact non-native surface materials (e.g., Si, $SiO_2$, TiN, polymeric resists, etc.). The activation of the precursor on such surfaces via reactive gas−solid collisions often dominates the growth process because the rates of steady-state growth on the native substrate are often much faster (that is to say, the reaction demonstrates a nucleation-limited autocatalysis). Although much progress has been made in determining the nature of steady-state CVD growth mechanisms, our understanding of the critical steps involved in activated nucleation is still quite limited.

A first step toward developing an understanding of a complex CVD process is to investigate the temperature-dependent surface chemistry of the precursor (or one of its possible reaction products). We employ an array of surface-specific analytical techniques, each appropriate to report on a given aspect of the mechanism. For example, Auger electron spectroscopy (AES),[17−19] X-ray photoelectron spectroscopy (XPS),[17,18] and low-energy electron diffraction (LEED)[20,21] are extremely useful methods with which to examine surface composition and order.

Temperature-programmed reaction spectroscopy (TPRS)[22−25] and reactive molecular beam surface scattering (MBSS)[15] are particularly useful for examining both the kinetics and reaction pathways of a CVD process. In a TPRS experiment, a cold surface is dosed once from the gas phase with a limited amount of an adsorbate. After dosing is complete, the surface is heated, causing various species (typically with different molecular masses) to desorb from the surface. The relative amount of each desorbing species is monitored as a function of surface temperature with a mass spectrometer. Typically, the TPRS traces reflect a convolution of the coverage and temperature dependencies of the surface reaction kinetics and, when modeled appropriately, can be used to determine the relevant reaction energetics.[23,26] The MBSS experiment is similar, except that the dosing of the surface

Elizabeth L. Crane received her B.A. degrees in chemistry and mathematics in 1995 from St. Olaf College. She is currently completing her Ph.D. degree at the University of Illinois at Urbana−Champaign.

Professor Gregory S. Girolami received his B.S. degrees in chemistry and physics from the University of Texas at Austin and his Ph.D. degree from the University of California at Berkeley. Thereafter, he was a NATO postdoctoral fellow with Sir Geoffrey Wilkinson at Imperial College of Science and Technology and joined the Illinois faculty in 1983.

Professor Ralph G. Nuzzo received his B.S. degree in chemistry from Rutgers University in 1976 and his Ph.D. degree in organic chemistry from the Massachusetts Institute of Technology in 1980. After completing his graduate studies, he accepted a position at Bell Laboratories, then a part of A.T.&T., where he held the title of Distinguished Member of the Technical Staff in Materials Research. He joined the Illinois faculty in 1991 and holds joint appointments in the Departments of Chemistry and Materials Science and Engineering.

10.1021/ar960102n CCC: $19.00 © 2000 American Chemical Society
Published on Web 09/27/2000

is done effusively and continues as the surface temperature is either raised or lowered. The composition of the scattered flux is measured as the function of temperature, and the resulting data provide information about the reaction energetics, reaction order, and product partitioning.

Both TPRS and MBSS are sensitive only to species that desorb into the gas phase. To study the structures of adsorbate species resident on the surface, surface vibrational spectroscopies are extremely powerful tools, and we have found reflection absorption infrared spectroscopy (RAIRS)[27-29] to be particularly useful.

In the sections that follow, we will discuss some representative mechanistic studies of CVD processes culled from our research. We will discuss how these studies may lead to improvements in CVD methods, and we will illustrate how additive fabrication based on selective CVD growth might find broader applications in technology. Several excellent reviews related to the material discussed here are available, and the interested reader is directed to them for more detailed discussions.[1,5,8]

## Unimolecular CVD Processes: Aluminum

**Aluminum CVD via the Thermolytic Decomposition of Triisobutylaluminum (TIBA).** One of the first CVD mechanisms we studied in depth was the deposition of aluminum thin films via the thermal decomposition of triisobutylaluminum (TIBA).[15] To model the steady-state growth behaviors, we avoided the complications of the nucleation steps by carrying out the reactions on a single crystalline aluminum surface. The mechanism of aluminum deposition from this precursor was poorly understood at the time, and the complex growth patterns limited the scope of its application in device fabrication.[13,30,31]

Reactive scattering studies were performed by directing an effusive beam of TIBA onto both Al(111) and Al(100) surfaces while simultaneously monitoring the desorbed and scattered species via mass spectroscopy. Figure 1 shows the results of these experiments on the Al(100) surface. The intensity of the $m/e = 141$ ion, a representative fragment of the TIBA precursor molecule, remains constant up to a temperature of ~500 K. At this point, the scattered flux decreases dramatically until reaching a background level at ~600 K. This result indicates that TIBA begins to react on the surface at a high rate at temperatures near 500 K (presumably depositing a film of aluminum). Concurrently, the fragments measured at $m/e = 56$ (isobutylene) and $m/e = 2$ (dihydrogen) increase; no intensity changes are seen at $m/e = 58$ (an isobutane fragment).

Taken together, these results suggest that the TIBA undergoes a surface-mediated reaction to give a metal deposit and the gaseous byproducts isobutylene and hydrogen. These results strongly suggest that an important step in the deposition process is $\beta$-hydrogen elimination from a surface-bound alkyl group.[15,32] TPRS studies also showed that the isobutylene and hydrogen are evolved from the decomposition of an adsorbed monolayer of

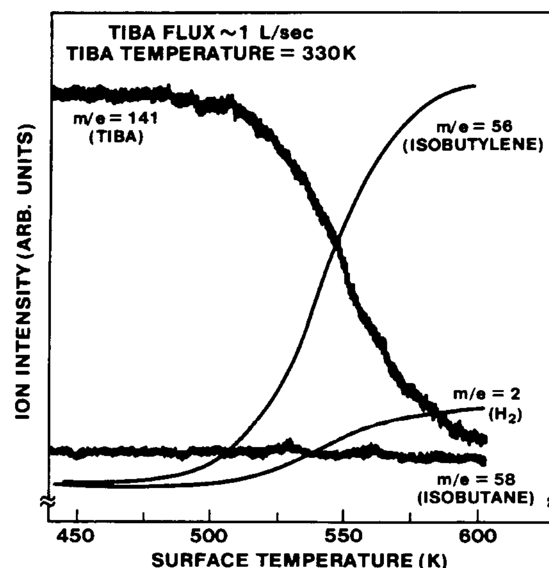


**FIGURE 1.** Scattered species as a function of surface temperature when TIBA ($T_{gas} = 330$ K) is impinged onto an Al(100) surface at an effective pressure of $10^{-6}$ Torr. The surface temperature is ramped linearly at ~2 K $s^{-1}$. The arbitrary units are different for each of the scattered fragments, which prohibits comparison of their relative intensities.

TIBA at ~520 K, in good agreement with the scattering data. Independent studies have shown that H atoms recombine and desorb as $H_2$ from aluminum surfaces at ~330 K,[33,34] and isobutylene desorbs from aluminum at ~130 K. Therefore, the evolution of these products at ~520 K in the thermolytic decomposition of TIBA must be a reaction-limited process, that is to say, one limited by the energetics of the $\beta$-hydrogen elimination step. The change in the ion profiles seen in the reactive scattering data above 600 K reflects the onset of a rate regime limited only by the TIBA flux.

Using AES, we determined that, below 600 K, the aluminum deposited on the surface remains carbon-free. Therefore, the CVD process occurring in this limited temperature range is quite efficient. At higher temperatures (>650 K), however, carbon contamination becomes a factor. Our subsequent studies strongly suggested that $\beta$-methyl elimination becomes a kinetically competent decomposition pathway above 600 K.[15] This deleterious side reaction leads to the evolution of propylene and the formation of methyl groups on the aluminum surface (which are known to dehydrogenate at $T \geq 400$ K).[35] These reaction steps are summarized in Figure 2. It is interesting to note that our data suggest that the barrier for $\beta$-methyl elimination is only ~4 kcal/mol higher than that for $\beta$-hydride elimination (see below), a result that mirrors the known reactivity differences of aluminum alkyls in homogeneous solution.[15]

Perhaps most intriguing was the presence of only one TPRS desorption feature for isobutylene. This result demonstrates that the decompositions of the three isobutyl groups in the adsorbed TIBA are kinetically indistinguishable. Thus, the dissociation of the TIBA into an

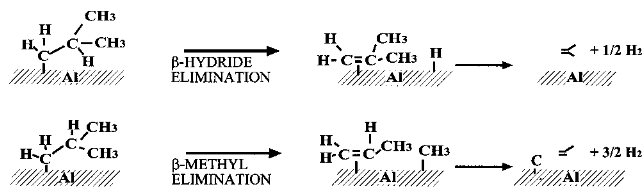


**FIGURE 2.** Proposed surface reaction mechanisms for the TIBA ligands on aluminum surfaces during steady-state aluminum CVD. For simplicity, the attached aluminum atoms are not shown. The $\beta$-hydrogen elimination reaction (top) dominates at surface temperatures <600 K and leads to carbon-free, crystalline aluminum films. We propose that the $\beta$-methyl elimination reaction (bottom) and subsequent $\alpha$-hydrogen abstractions from the surface methyl group are the source of carbon incorporation into aluminum films deposited above 600 K.

adsorbed Al atom and three kinetically equivalent isobutyl groups must take place below 520 K (i.e., dissociative adsorption is not the rate-determining step).

The activation energy and preexponential factor of the rate-limiting $\beta$-hydrogen elimination can be obtained from a Redhead analysis of TPRS data taken at different temperature ramp rates.[26] An activation energy of 27.2 kcal mol$^{-1}$ and a preexponential factor of $3.8 \times 10^{11}$ s$^{-1}$ were found for the production of isobutylene on Al (111). For the (100) surface, these quantities were 32.6 kcal mol$^{-1}$ and $1.4 \times 10^{13}$ s$^{-1}$. These data demonstrate that a marked surface rate–structure sensitivity favoring the growth of the (111) face operates in this CVD system. The energetics measured here do, in fact, completely rationalize the strong (111) texture seen in CVD growth from TIBA in commercial reactors.[13]

**Trimethylamine Alane (TMAA).** Trialkylamine alanes, specifically trimethylamine alane (TMAA), have also proven useful as precursors for aluminum thin films.[36] The primary advantage of TMAA over TIBA is that aluminum deposition can be effected at lower temperatures. TMAA is relatively stable and has a reasonably high vapor pressure at room temperature, making it a good choice for use in CVD.[37,38] AES verified that high-purity Al films are obtained from TMAA, and LEED data showed that the growth proceeds epitaxially on both (100) and (111) Al surfaces.

The major products derived from the decomposition of TMAA (besides Al metal) are trimethylamine (TMA) and molecular hydrogen, both of which bind only weakly to the growth surface and thus desorb with a high rate. Our TPRS data suggested that the kinetics of the deposition are limited by the rate of heterolytic cleavage of the Al–N bond of adsorbed TMAA molecules.[36] Reactive scattering studies at a variety of precursor fluxes (Figure 3) were consistent with this conclusion: the deposition rate at low temperatures was first-order in precursor, and the decomposition of the precursor was characterized by a preexponential factor of $3 \times 10^{12}$ s$^{-1}$ and an activation energy of 17.8 kcal mol$^{-1}$. This barrier is some 9.4 kcal/mol lower than that of the TIBA CVD process.

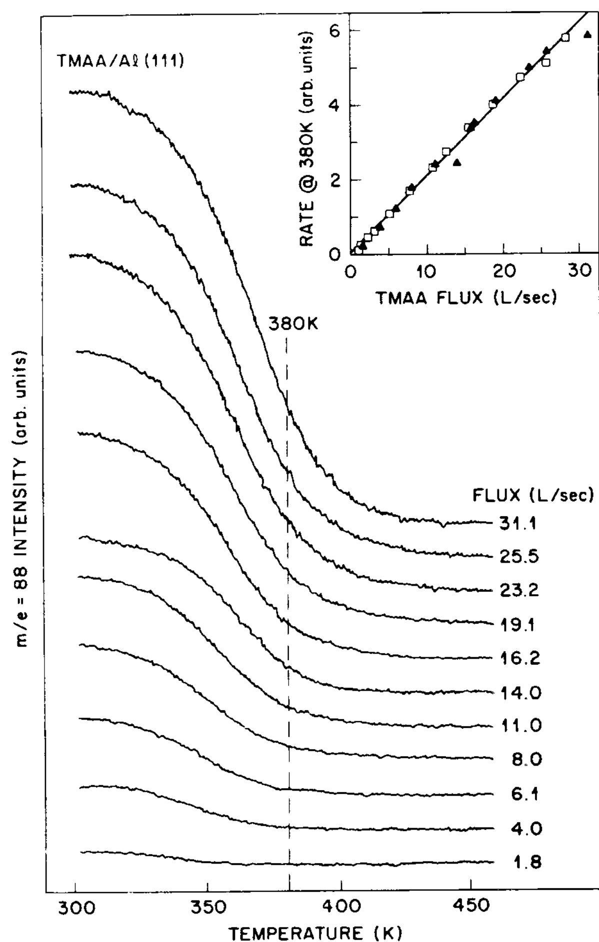


**FIGURE 3.** Scattering profiles of trimethylamine alane from clean Al(111) as a function of temperature and with varying gas flux. The heating rate is 4 K s$^{-1}$. The inset shows that the decomposition reaction is first-order in TMAA flux on both Al(111) (▲) and Al(100) (□).

The deposition kinetics can be modeled by a mechanism consisting of the following discrete steps:

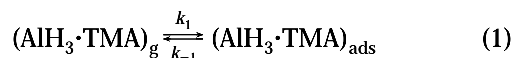

$$(\mathrm{AlH_3{\cdot}TMA})_g \underset{k_{-1}}{\overset{k_1}{\rightleftharpoons}} (\mathrm{AlH_3{\cdot}TMA})_{ads} \quad (1)$$

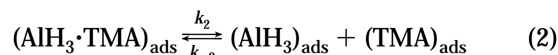

$$(\mathrm{AlH_3{\cdot}TMA})_{ads} \underset{k_{-2}}{\overset{k_2}{\rightleftharpoons}} (\mathrm{AlH_3})_{ads} + (\mathrm{TMA})_{ads} \quad (2)$$

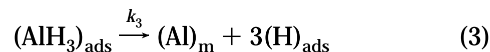

$$(\mathrm{AlH_3})_{ads} \xrightarrow{k_3} (\mathrm{Al})_m + 3(\mathrm{H})_{ads} \quad (3)$$

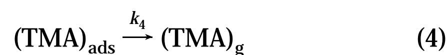

$$(\mathrm{TMA})_{ads} \xrightarrow{k_4} (\mathrm{TMA})_g \quad (4)$$

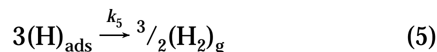

$$3(\mathrm{H})_{ads} \xrightarrow{k_5} {}^3/_2(\mathrm{H_2})_g \quad (5)$$

where the subscripts g, ads, and m refer to the gas, adsorbed, and metal phases, respectively. In principle, the non-flux-limited reaction rate should be controlled either by the surface-mediated cleavage of the Al–N bond in TMAA ($k_2$) or by the recombinative desorption of hydrogen ($k_5$). The 17.8 kcal mol$^{-1}$ activation energy and the first-order reaction kinetics are inconsistent with the known

kinetics of H atom recombination, and strongly suggest that Al−N bond cleavage is the rate-determining step ($k_2$).

## A Bimolecular CVD Process: Redox Transmetalation

TIBA and TMAA both afford an elementary phase Al, as a CVD product. Compositionally more complex materials, however, are often used in industrial applications; for example, alloys are frequently used to combine the favorable aspects of two different metals (e.g., aluminum/copper to optimize conductivity and resistance to electromigration).[39−42] We have been broadly interested in the deposition of Cu and its alloys, and toward this end we have examined the CVD reactions of several metal diketonate complexes on copper surfaces. We highlight in this Account one alloy CVD system that demonstrates remarkable properties.

**Transmetalation of Pd(hfac)$_2$ on a Copper Surface.** Preliminary studies of bis(hexafluoroacetylacetonate)-palladium(II), Pd(hfac)$_2$, on polycrystalline copper substrates revealed that the deposition of Pd occurs via a redox transmetalation reaction as shown below:[3,39,43]

$$\mathrm{Pd(hfac)_2 + Cu \rightarrow Pd + Cu(hfac)_2} \qquad (6)$$

Detailed mechanistic studies demonstrated that Pd(hfac)$_2$ readily dissociates on a clean copper surface and that this reaction leads to the formation of Cu(hfac)$_2$ at temperatures between 330 and 600 K. Our studies showed that the transmetalation reaction involves six principal steps: (1) the adsorption of the Pd(hfac)$_2$ molecules on the surface, (2) the reduction of the Pd$^{II}$ centers to Pd$^0$ by copper, (3) the dissociation of the hfac ligands from the palladium centers, (4) the recombination of hfac with copper surface atoms, (5) the reaction-limited desorption of Cu(hfac)$_2$, and (6) the interdiffusion of palladium into the copper substrate.

XPS studies indicated that, upon adsorption of the precursor on Cu, even at low temperatures (∼120 K), the measured Pd 3d$_{5/2}$ binding energy corresponds to that of Pd$^0$ rather than Pd$^{II}$. This result suggests that the palladium(II) centers of the adsorbate are reduced readily by the copper surface. Adsorption of Pd(hfac)$_2$ evidently occurs dissociatively; i.e., the hfac ligands transfer from Pd to the Cu surface. The RAIR spectra shown in Figure 4 show significant dichroism that can only be rationalized by a tilt-order transition of the surface-bound hfac ligands near 300 K. In this transition, the hfac ligands, whose molecular planes initially are mostly parallel to the surface plane, reorient and become perpendicular to the surface. The latter organizational state persists until the ligands begin to decompose (∼500 K). That the hfac ligands remain intact on the surface up to temperatures near 500 K was further supported by the XPS data.

Extensive kinetic studies were conducted to demonstrate the controlling effects of diffusion in the solid state on this novel reaction (Figure 5). To facilitate interdiffusion, a polycrystalline Cu substrate was used in this experiment. The data in the figure show that both Cu-

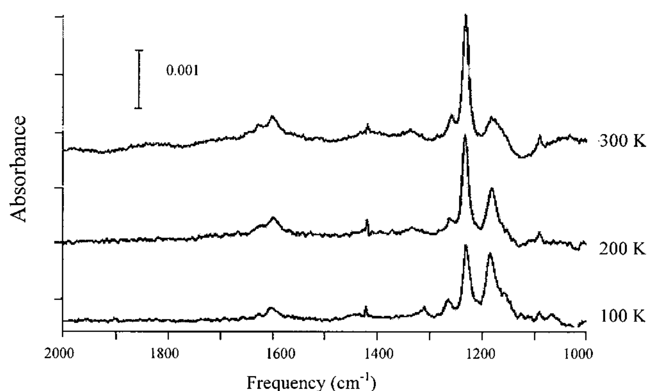


**FIGURE 4.** RAIR spectra of submonolayer amounts of Pd(hfac)$_2$ on a Cu(111) surface after the surface was annealed to different temperatures.

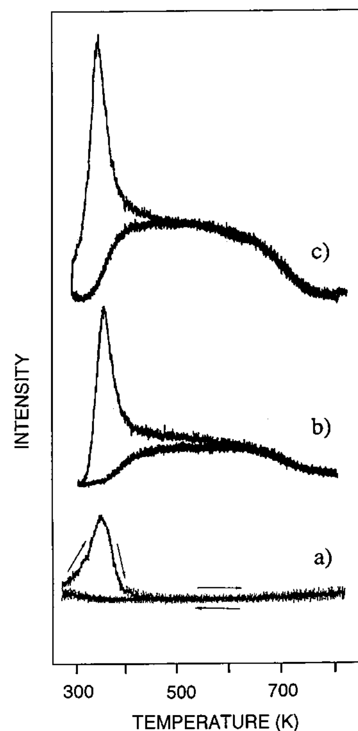


**FIGURE 5.** Profiles obtained during the reactive scattering of Pd(hfac)$_2$ on copper foil surfaces: (a) $m/e = 244$, which tracks the desorption of Pd(hfac)$_2$, (b) $m/e = 201$, which tracks the desorption of Cu(hfac)$_2$, and (c) $m/e = 201$ but at twice the incident flux of Pd(hfac)$_2$. For (a) and (b) the flux was $5 \times 10^{13}$ molecules cm$^{-2}$ s$^{-1}$; for (c) the flux was $1 \times 10^{14}$ molecules cm$^{-2}$ s$^{-1}$. The heating rates were 7 K s$^{-1}$. The arrows indicate whether the traces were obtained upon heating or cooling. In both curves, the lowest signal corresponds to zero flux.

(hfac)$_2$ and Pd(hfac)$_2$ are present in the desorbing flux at temperatures between 300 and 400 K. Above 400 K, however, the Pd(hfac)$_2$ intensity drops dramatically as it is more quantitatively converted to products. Above 400 K, the reaction rate is limited by the flux of Pd(hfac)$_2$ to the surface. This conclusion is corroborated by the increased yields of Cu(hfac)$_2$ obtained at higher Pd(hfac)$_2$ fluxes. The decrease in Cu(hfac)$_2$ intensity seen at higher temperatures is due to the onset of the thermal decomposition of the hfac ligands on the surface. This latter

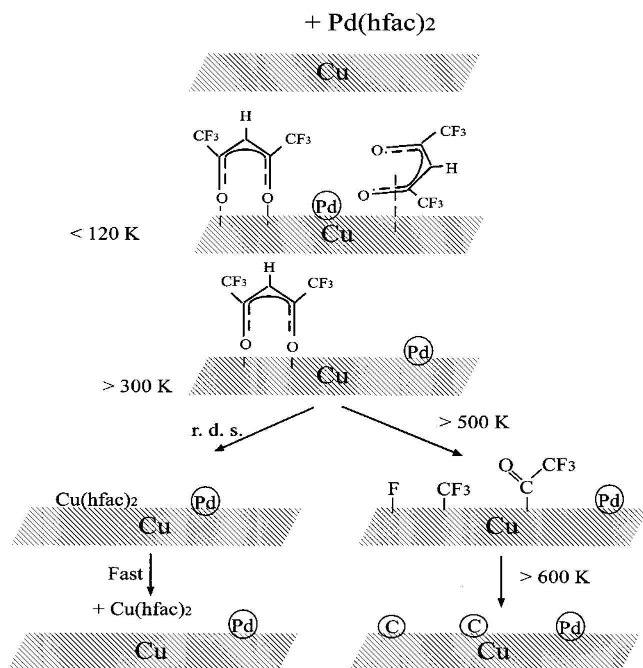


**FIGURE 6.** Overall mechanism for the transmetalation of $Pd(hfac)_2$ on copper surfaces under CVD conditions.

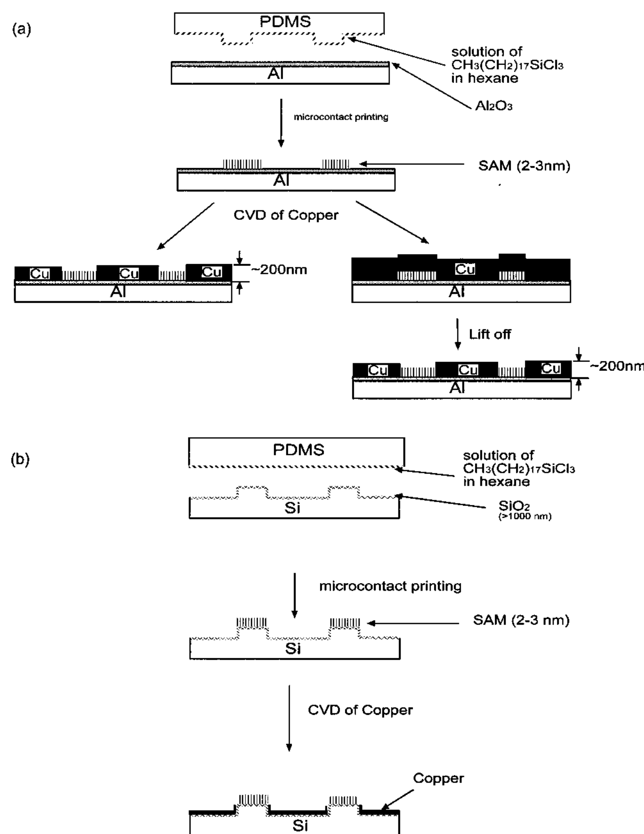


**FIGURE 7.** Schematic outline of the procedures for patterning alkylsiloxanes on a planar (a) and a nonplanar (b) substrate. Nucleation and deposition of copper occur only on those regions underivatized by the SAM.

branching necessarily limits the yield of the $Cu(hfac)_2$ transmetalation product. The overall process is depicted in Figure 6.

The kinetics revealed by the reactive scattering experiments can be analyzed in considerable detail. Based on well-supported simplifying assumptions, the ratio of the $Cu(hfac)_2$ desorbed to the incident $Pd(hfac)_2$ flux can be written in terms of the energetics of the various elementary rate processes involved in the competing reactions. From this model, using a least-squares analysis to fit the data, we were able to estimate that the activation energy for the transmetalation reaction was remarkably small: 13 kcal $mol^{-1}$ (with a corresponding preexponential factor of $2 \times 10^{-10}$ $molecules^{-1}$ $cm^2$ $s^{-1}$). The data are consistent with known temperature dependencies of the diffusion of Pd into Cu.

In principle, the redox transmetalation process can serve as a method to deposit metals selectively; for example, if $Pd(hfac)_2$ is passed over a substrate that consists of regions of various compositions—copper here, silicon there, etc.—palladium metal will only be deposited on the copper. This selectivity arises because few materials (copper being one) are able to reduce the $Pd^{II}$ ions in the precursor to palladium metal. This approach to effecting patterned or surface-selective depositions, however, relies on a preexisting pattern of surface compositions. A much more widely applicable approach to obtaining patterned metal thin films is described in the following section.

## New Approaches to Patterning CVD Metal Thin Films[44]

Many metal CVD depositions are autocatalytic. Growth of such thin films is characterized by an induction period, which is a consequence of the higher barriers that pertain to the activation of the precursor on a non-native substrate. This dependence of the nucleation rate on the nature of the surface is the basis of powerful new approaches to control CVD metalization processes. In principle, a surface tailored to present regions that inhibit and promote the nucleation step should lead to an intrinsically patterned (i.e., additive) deposition. We have broadly explored the utility of molecular thin films, and self-assembled monolayers (SAMS) in particular, as one means of doing this. Numerous methods for patterning SAMS have been described,[45−52] but none is as easy or as generally useful as microcontact printing ($\mu$-CP),[14,48−50,53] a method uniquely suited to creating diverse chemical environments on a sample surface.

The basis of $\mu$-CP as a patterning method for CVD is illustrated in Figure 7. Using a functional ink, $\mu$-CP can deposit patterned SAMs on essentially any type of substrate material. In our work, we have made extensive use of SAMs derived from organosilicon coupling agents in conjunction with CVD to deposit metal films selectively in a self-registering pattern.[50,53−55] Most typically, stamps constructed of poly(dimethylsiloxane) (PDMS) were "inked" with a solution of octadecyltrichlorosilane (OTS). The stamp was placed in brief contact with a Si(100) wafer or other substrate, leaving behind a monolayer of the alkylsiloxane. Dense OTS SAMs, which take hours or more to assemble from solution,[56−59] can be deposited in less than

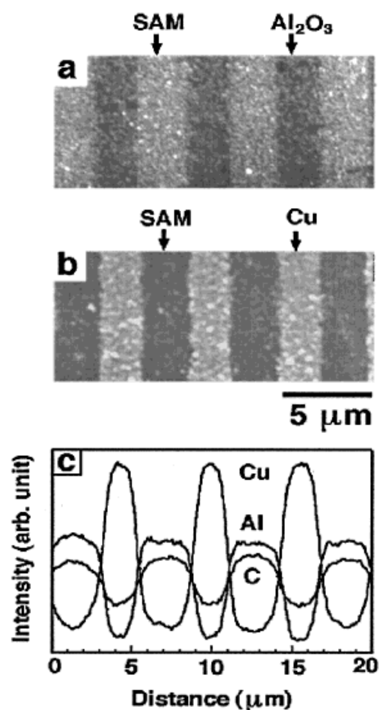


**FIGURE 8.** (a) Scanning electron micrograph of patterned SAMs of octadecylsiloxane (parallel lines, 3 $\mu$m in width and separated by 2 $\mu$m) on the surface of $Al/Al_2O_3$. (b) Scanning electron micrograph of lines of copper (2 $\mu$m in width and ~200 nm in thickness) deposited by selective CVD on the same patterned surface shown in (a). The bright regions correspond to the lines of copper. (c) Auger electron spectroscopy (AES) line scans on the samples of (b) in the direction perpendicular to the lines of copper.

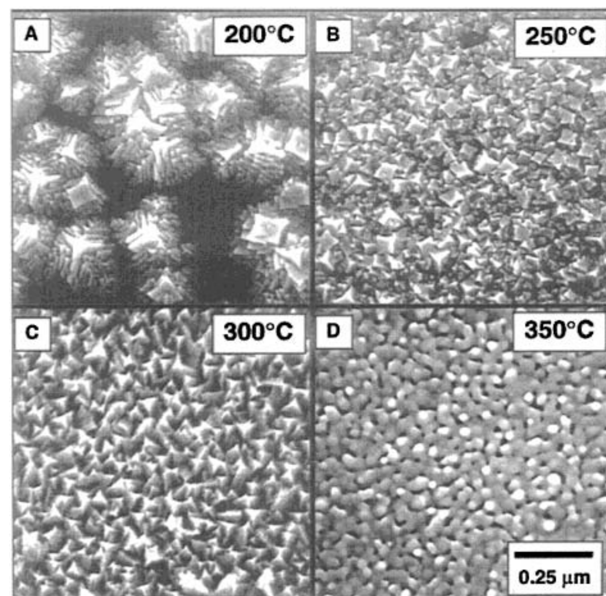


**FIGURE 9.** Scanning electron micrographs of platinum films deposited at different tempearatrues on TiN substrates. The Ar and $H_2$ flow ratios were fixed at 50 and 20 sccm, respectively. All depositions were carried out in the presence of water vapor at a total chamber pressure of 0.5 Torr.

1 min by $\mu$-CP.[14,60] A suitable CVD precursor is then passed at moderate temperatures (usually less than 350 °C) over the surface bearing the SAM. Deposition of the metal occurs only in areas not covered by the SAM (this approach to patterned metalization is termed orthogonal additive deposition). Even if the nucleation rates on the modified and unmodified surface regions are similar, so that the deposition is nonselective, patterned metalization can still be effected because the SAM can serve as a lift-off mask.

Figure 8 shows the results of an early study of direct patterning by Cu CVD. The SEM image shows a patterned monolayer of OTS deposited by $\mu$-CP on an $Al/Al_2O_3$ substrate (Figure 8a). This surface was then exposed to Cu(hfac)(vtms)—a CVD precursor that was used to deposit a 0.1-$\mu$m-thick copper film on the surface. Figure 8b shows that the deposition occurs selectively on those parts of the surface not covered with the SAM. Figure 8c makes this selectivity more obvious: the AES line scan shows that the OTS regions are essentially devoid of copper. More recent studies have shown that the defect densities can be reduced markedly from the levels demonstrated in this figure (by at least several orders of magnitude).

**Control of the Selectivity and Morphology in CVD Thin Films.** There is a great current need to develop new methods to control the morphology of a metal film microstructure fabricated by CVD.[61] Generally speaking, we have only begun to develop a rudimentary understanding of how the deposition chemistries can be manipulated to effect better control over the structural habits and crystallographic textures obtained. The dimensions of this challenge are illustrated by a study of the deposition of Pt from the hexafluoroacetylacetonate precursor, $Pt(hfac)_2$. This study answered questions not only about the efficacy of $\mu$-CP as a method to effect patterned deposition but also about the influence of deposition parameters on nucleation and subsequent grain growth.

Deposition of Pt from $Pt(hfac)_2$ requires the addition of $H_2$ as a reductant. If this mixture is passed over $SiO_2$ or TiN substrates treated by $\mu$-CP with OTS, platinum deposition occurs selectively on the unmodified substrate over a wide temperature range (from essentially room temperature to 350 °C), provided that the flux of $Pd(hfac)_2$ is kept low. If the flux is raised to sustain growth rates of Pt above 400 Å/min, however, the growth is less selective.

The platinum thin films actually consist of a mat of intergrown, faceted crystals. This morphology is generally undesirable in technological applications, smooth films being preferred. We found that addition of water vapor to the gas flux increased the number of nucleation sites, so that the platinum grains were smaller and the film was more uniform. The morphology of the deposit changed significantly upon raising the temperature of the substrate, as long as sufficient water vapor was added to maintain the nucleation density in the non-OTS-bearing regions. As shown in Figure 9, at low temperatures (200 °C, Figure 9A) the film consists of highly faceted grains. At higher temperatures, the films obtained are smoother although still obviously faceted. Intriguingly, above 325 °C, the grains become round and the surfaces smooth. This latter result proved to be of particular importance because it made possible the self-aligned multilevel fabrication of

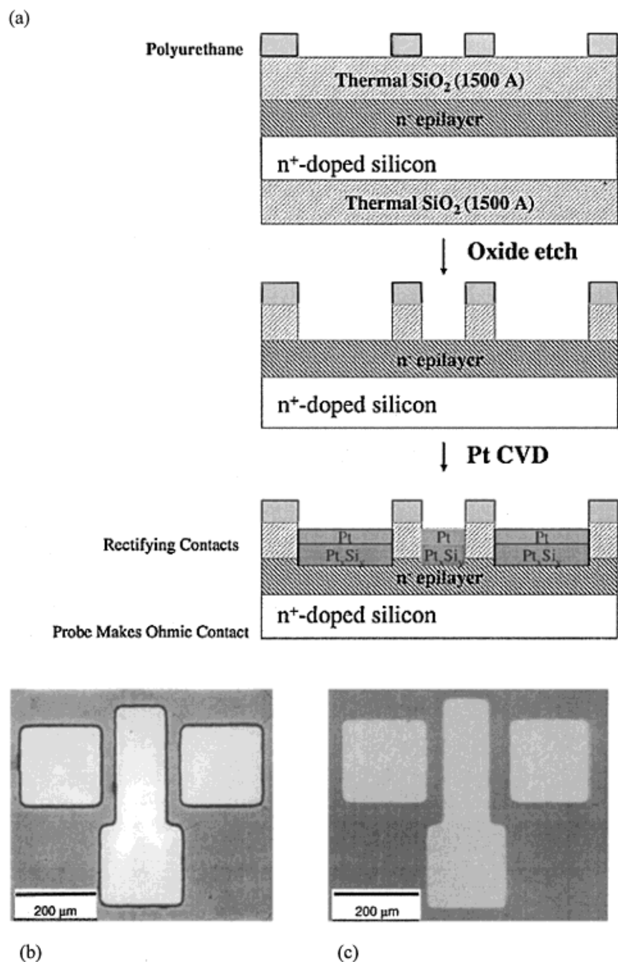


**FIGURE 10.** (a) Schematic of diode fabrication steps. The polyurethane is deposited on the silicon substrate by spreading through recessed areas of a patterned poly(dimethylsiloxane) mold. (b) Optical micrograph of diodes fabricated by the method shown in Figure 1 before removal of the polyurethane layer. (c) Optical micrograph of diodes fabricated by the method shown in Figure 1 after removal of the polyurethane layer.

lead zirconium titanate (PZT) ferroelectric capacitor arrays, in which additively patterned platinum was used as the contact electrodes.[61]

## Additive CVD Fabrication of Electronic Devices

In the past few years, we have shown that additive fabrication methods can be used to generate a variety of multilevel thin-film assemblies and devices, including ferroelectric capacitors[61] and MOSFET devices.[16] Much of this work has also addressed the development of soft lithography[62] as a natural component of this fabrication method. We have not tried to push the limits of the feature sizes that can be reached. Rather, our interests have centered on developing the chemistries of additive patterning and demonstrating how they can be directly linked to the soft-lithography-based fabrication of multilayer architectures. Since many of these architectures require multilevel registration, we have generally adopted design rules in the 10−100-$\mu$m size range to facilitate the laboratory-scale demonstration, and thus potential utility, of these new techniques.

We conclude this Account with a description of the fabrication of Pt−Si Schottky diodes[63] as a representative example of how selective CVD can be used to construct multicomponent devices. Figure 10 depicts the fabrication steps necessary for the assembly of this diode structure. In the first step, a patterned polyurethane resist was formed on a thick thermal oxide ($SiO_2$) layer on a silicon-(100) wafer. The resist was formed by means of micromolding in capillaries (MIMIC), a soft lithography patterning method described by Xia, Kim, and Whitesides.[64,65] Holes in the oxide were then opened using a wet etch. The wafer was then placed in the CVD reactor and exposed to $Pt(hfac)_2$ in the presence of $H_2$; water was added to the feed during the early stages of deposition to assist the nucleation. As the figure shows, the polymer resist strongly directs both the etching and the Pt deposition steps. At the temperature at which this deposition was carried out (573 K), interdiffusion yields a layer of $Pt_x$-$Si_y$ at the interface between the silicon wafer and the platinum film. RBS and Auger depth profiling revealed that a graded compositional profile is present in this intermetallic layer. The diodes showed *IV* characteristics expected for these silicide junctions.[63]

## Concluding Remarks

Chemical vapor deposition is an extremely useful process. Its advantages include versatility, the potential for selectivity, improved conformal coverages, and low processing temperatures. We believe that additive CVD fabrication methods could provide an attractive alternative to traditional patterning techniques, which involve sequential blanket depositions of thin films followed by a subtractive etching process. In addition, techniques such as additive CVD that minimize waste will become increasingly important in a "green"-conscious manufacturing environment.

We hope the examples discussed here illustrate the complexities of the surface chemistries involved in CVD systems and the opportunities CVD presents for progress in research and manufacturing.

*Our research has benefited from the support of many people and institutions. We thank the National Science Foundation, Department of Energy, and Defense Advanced Research Project Agency for financial support. Special recognition goes to Lawrence Dubois and the late Brian Bent, two friends and collaborators without whom we would have been lost, and to Nooli Jeon, Martin Erhardt, and Wenbin Lin, past and current graduate students at UIUC.*

## References

(1) Jensen, K. S.; Kern, W. In *Thin Film Processes*; Vossen, J. L., Kern, W., Eds.; Academic: Boston, 1991; Vol. II, pp 283−353.
(2) Tagge, C. D.; Simpson, R. D.; Bergman, R. G.; Hostetler, M. J.; Girolami, G. S.; Nuzzo, R. G. Synthesis of a Novel Volatile Platinum Complex for Use in CVD and a Study of the Mechanism of Its Thermal Decomposition in Solution. *J. Am. Chem. Soc.* **1996**, *118*, 2634−2643.
(3) Lin, W.; Warren, T. H.; Nuzzo, R. G.; Girolami, G. S. Surface-Selective Deposition of Palladium and Silver Films from Metal−

Organic Precursors: A Novel Metal−Organic Chemical Vapor Deposition Redox Transmetalation Process. *J. Am. Chem. Soc.* **1993**, *115*, 11644−11645.
(4) Jeon, N. L.; Lin, W.; Erhardt, M. K.; Girolami, G. S.; Nuzzo, R. G. Selective Chemical Vapor Deposition of Platinum and Palladium Directed by Monolayers Patterned Using Microcontact Printing. *Langmuir* **1997**, *13*, 3833−3838.
(5) Powell, C. F.; Oxley, J. H.; Blocher, J. M., Jr. *Vapor Deposition*; Wiley: New York, 1966; pp 256−257.
(6) Voorhoeve, R. J. H.; Merewether, J. W. Selective Deposition of Silver on Silicon by Reaction with Silver Fluoride Vapor. *J. Electrochem. Soc.* **1972**, *119*, 364−368.
(7) Tsao, K. Y.; Busta, H. H. Low-Pressure Chemical Vapor Deposition on Polycrystalline and Single Crystal Silicon via the Silicon Reduction. *J. Electrochem. Soc.* **1984**, *131*, 2702−2708.
(8) Kodas, T. T.; Hampden-Smith M. J. *Chemistry of Metal CVD*; VCH: New York, 1994; and references therein.
(9) Shin, H. K.; Chi, K. M.; Hampden-Smith, M. J.; Kodas, T. T.; Farr, J. D.; Paffett, M. Selective Low-Temperature Chemical Vapor Deposition of Copper from Hexafluoroacetylacetonato copper(I) trimethylphosphine, (hfa)CuP$(Me)_3$ *Adv. Mater.* **1991**, *3*, 246−248.
(10) Norman, J. A. T.; Muratore, B. A.; Dwyer, D. N.; Roberts, D. A.; Hochberg, A. K. New OMCVD Precursors for Selective Metallization. *J. Phys. IV* **1991**, *1* (C2), 271−278.
(11) Chi, K. M.; Garvey, J. W.; Shin, H. K.; Hampden-Smith, M. J.; Kodas, T. T.; Farr, J. D.; Paffett, M. F. Chemical Vapor Deposition via Disproportionation of Hexafluoroacetylacetanato(1,5-cyclooctadiene)Copper(I) (hfac)Cu(1,5-COD). *J. Mater. Res.* **1991**, *7*, 261−264.
(12) Dubois, L. H.; Zegarski, B. R. Selectivity and Copper Chemical Vapor Deposition. *J. Electrochem. Soc.* **1992**, *139*, 3295−3299.
(13) Green, M. L.; Levy, R. A.; Nuzzo, R. G.; Coleman, E. Aluminum Films Prepared by Metal−Organic Low Pressure Chemical Vapor Deposition. *Thin Solid Films* **1984**, *114*, 367−377.
(14) Jeon, N. L.; Nuzzo, R. G.; Xia, Y.; Mrksich, M.; Whitesides, G. M. Patterned Self-Assembled Monolayers Formed by Microcontact Printing Direct Selective Metalization by Chemical Vapor Deposition on Planar and Nonplanar Substrates. *Langmuir* **1995**, *11*, 3024−3026.
(15) Bent, B. E.; Nuzzo, R. G.; Dubois, L. H. Surface Organometallic Chemistry in the Chemical Vapor Deposition of Aluminum Films Using Triisobutylaluminum: $\beta$-Hydride and $\beta$-Alkyl Elimination Reactions of Surface Alkyl Intermediates. *J. Am. Chem. Soc.* **1989**, *111*, 1634−1644.
(16) Jeon, N. L.; Clem, P.; Jung, D. Y.; Lin, W. B.; Girolami, G. S.; Payne, D. A.; Nuzzo, R. G. Additive Fabrication of Integrated Ferroelectric Thin-Film Capacitors Using Self-Assembled Organic Thin-Film Templates. *Adv. Mater.* **1997**, *9*, 891−895.
(17) Powell, C. J. Compositional Analyses of Surfaces and Thin Films by Electron and Ion Spectroscopies. *Crit. Rev. Surf. Chem.* **1993**, *2*, 17−35.
(18) Bringgs, D., Seah, M. P., Eds. *Practical Surface Analysis by Auger and Photoelectron Spectroscopy*; Wiley: New York, 1987.
(19) Briant, C. L.; Messner, R. P. *Auger Electron Spectroscopy*; Academic Press: Troy, MO, 1988.
(20) Van Hove, M. A.; Weinberg, W. H.; Chan, C.-M. *Low Energy Electron Diffraction*; Springer: Berlin, 1986.
(21) Van Hove, M. A. *MSA Bull.* **1993**, *23*, 119.
(22) King, D. A. Thermal Desorption from Metal Surfaces: A Review. *Surf. Sci.* **1975**, *47*, 384−402.
(23) Parker, D. H.; Jones, M. E.; Koel, B. E. Determination of the Reaction Order and Activation Energy for Desorption Kinetics Using TPD Spectra: Application to $D_2$ Desorption from Ag(111). *Surf. Sci.* **1990**, *233*, 65−74.
(24) Chan, C.-M.; Aris, R.; Weinberg, W. H. *Appl. Surf. Sci.* **1978**, *1*, 360.
(25) Schlichting, H.; Menzel, D. Techniques for Wide-Range, High Resolution and Precision Thermal Desorption Measurements 1. Principles of Apparatus and Operation. *Surf. Sci.* **1993**, *285*, 209−218.
(26) Redhead, P. A. Thermal Desorption of Gases. *Vacuum* **1962**, *12*, 203-211.
(27) Francis, S. A.; Ellison, A, H. Infrared Spectra of Monolayers on Metal Mirrors. *J. Opt. Soc. Am.* **1959**, *49*, 131−138.
(28) Greenler, R. G. Infrared Study of Adsorbed Molecules on Metal Surfaces by Reflection Techniques. *J. Chem. Phys.* **1966**, *44*, 310−315.
(29) Chabal, Y. L. Surface Infrared Spectroscopy. *Surf. Sci. Rep.* **1988**, *8*, 211−357.
(30) Cooke, M. J.; Heineke, R. A.; Stern, R. C.; Maes, J. W. C. *Solid State Technol.* **1984**, *25*, 62.
(31) Levy, R. A.; Green, M. L.; Gallegher, P. K. Characterization of LPCVD Aluminum for VLSI Processing. *J. Electrochem. Soc.* **1984**, *131*, 2175−2182.
(32) Bent, B. E.; Nuzzo, R. G.; Zegarski, B. R.; Dubois, L. H. Thermal Decomposition of Alkyl Halides on Aluminum. 1. Carbon−Halogen Bond Cleavage and Surface $\beta$-Hydride Elimination Reactions. *J. Am. Chem. Soc.* **1991**, *113*, 1137−1142.
(33) Paul, J.; Hoffmann, F. M. Hydrogen Adsorption on Alkali Modified Aluminum. *Surf. Sci.* **1988**, *194*, 419−437.
(34) Paul, J. Hydrogen Adsorption on Al(100). *Phys. Rev. B* **1988**, *37*, 6164−6173.
(35) Chen, J. G.; Beebe, T. P., Jr.; Crowell, J. E.; Yates, J. T., Jr. Reaction of Atomically Clean Aluminum and Chemically Modified Aluminum with Alkyl Halides. *J. Am. Chem. Soc.* **1987**, *109*, 1726−1729.
(36) Dubois, L. H.; Zegarski, B. R.; Kao, C.-T.; Nuzzo, R. G. The Adsorption and Thermal Decomposition of Trimethylamine Alane on Aluminum and Silicon Single-Crystal Surfaces: Kinetic and Mechanistic Studies. *Surf. Sci.* **1990**, *236*, 77−84.
(37) Gladfelter, W. L.; Boyd, D. C.; Jensen, K. F. Trimethyl Amine Complexes of Alane as Precursors for the Low Pressure Chemical Vapor Deposition (LPCVD) of Aluminum. *Chem. Mater.* **1989**, *1*, 339−343.
(38) Simmonds, M. G.; Phillips, E. C.; Hwang, J.-W.; Gladfelter, W. L. A Stable, Liquid Precursor for Aluminum. *Chemtronics* **1991**, *5*, 155−158.
(39) Lin, W.; Wiegand, B. C.; Nuzzo, R. G.; Girolami, G. S. Mechanistic Studies of Palladium Thin Film Growth from Palladium(II) $\beta$-Diketonates. 1. Spectroscopic Studies of the Reactions of Bis(hexafluoroacetylacetonato)palladium(II) on Copper Surfaces. *J. Am. Chem. Soc.* **1996**, *118*, 5977−5987.
(40) Girolami, G. S.; Jeffries, P. M.; Dubois, L. H. Mechanisitc Studies of Copper Thin-Film Growth from $Cu^I$ and $Cu^{II}$ $\beta$-Diketonates. *J. Am. Chem. Soc.* **1993**, *115*, 1015−1024.
(41) Shingubara, S.; Nakasaki, Y.; Kaneko, H. Electromigration in Single-Crystal Submicron Width Aluminum Interconnection. *Appl. Phys. Lett.* **1991**, *58*, 42−44.
(42) Kang, H. K.; Chen, J.; Asano, I.; Wong, S. *Proceedings, VMIC Conference*, June 1992
(43) Lin, W.; Nuzzo, R. G.; Girolami, G. S. Mechanistic Studies of Palladium Thin Film Growth from Palladium(II) $\beta$-Diketonates. 2. Kinetic Analysis of the Transmetalation Reaction of Bis(hexafluoroacetylacetonato)palladium(II) on Copper Surfaces. *J. Am. Chem. Soc.* **1996**, *118*, 5988−5996.
(44) Kaloyeros, A. E.; Fury, M. A. Chemical Vapor Deposition of Copper for Multilevel Metallization. *MRS Bull.* **1993**, *18*, 22−29.
(45) Calvert, J. M. In *Lithographically Patterned Self-Assembled Films*; Ulman, A., Ed.; Academic: San Diego, CA, 1993; Vol. 20, pp 109−141.
(46) Dulcey, C. S.; Georger, J. H.; Krauthamer, V.; Fare, T. L.; Stenger, D. A.; Calvert, J. M. Deep UV Photochemistry of Chemisorbed Monolayers: Patterned Coplanar Molecular Assemblies. *Science* **1991**, *252*, 551−554.
(47) Potochnik, S. J.; Pehrsson, P. E.; Hsu, D. S. Y.; Calvert, J. M. Selective Copper Chemical Vapor Deposition Using Pd-Activated Organosilane Films. *Langmuir* **1995**, *11*, 1841−1845.
(48) Kumar, A.; Biebuyck, H. A.; Abbott, N. L.; Whitesides, G. M. The Use of Self-Assembled Monolayers and a Selective Etch to Generate Patterned Gold Features. *J. Am. Chem. Soc.* **1992**, *114*, 9188−9189.
(49) Kumar, A.; Whitesides, G. M. Features of Gold Having Micrometer to Centimeter Dimensions Can Be Formed Through a Combination of Stamping with an Elastomeric Stamp and an Alkanethiol Ink Followed by Chemical Etching. *Appl. Phys. Lett.* **1993**, *63*, 2002−2004.
(50) Kumar, A.; Biebuyck, H. A.; Whitesides, G. M. Patterning Self-Assembled Monolayers−Applications in Materials Science. *Langmuir* **1994**, *10*, 1498−1511.
(51) Xia, Y.; Zhao, X.; Whitesides, G. M. Pattern Transfer−Self-Assembled Monolayers as Ultrathin Resists. *Microelectron. Eng.* **1996**, *32*, 255−268.
(52) Ross, C. B.; Sun, L.; Crooks, R. M. Scanning Probe Lithography 1. Scanning Tunneling Microscope Induced Lithography of Self-Assembled n-Alkanethiol Monolayer Resists. *Langmuir* **1993**, *9*, 632−636.
(53) Xia, Y.; Mrksich, M.; Kim, E. Microcontact Printing of Octadecylsiloxane on the Surface of Silicon Oxide and Its Applications in Microfabrication. *J. Am. Chem. Soc.* **1995**, *117*, 9576−9577.
(54) Wilbur, J. L.; Kumar, A.; Kim, E.; Whitesides, G. M. Microfabrication by Microcontact Printing of Self-Assembled Monolayers. *Adv. Mater.* **1994**, *6*, 600−604.
(55) Jeon, N. L.; Clem, P. G.; Payne, D. A.; Nuzzo, R. G. A Monolayer-Based Lift-Off Process for Patterning Chemical Vapor Deposition Copper Thin Films. *Langmuir* **1996**, *12*, 5350−5355.
(56) Wasserman, S. R.; Tao, Y. T.; Whitesides, G. M. Structures and Reactivity of Alkylsiloxane Monolayers Formed by Reaction of

Alkyltrichlorsilane on Silicon Substrates. *Langmuir* **1989**, *5*, 1074−1087.
(57) Gun, J.; Iscovici, R.; Sagiv, J. On the Formation and Structure of Self-Assembling Monolayers. *J. Colloid Interface Sci.* **1984**, *101*, 201−213.
(58) Parikh, A. N.; Allara, D. L.; Azonz, I. B.; Rondelez, F. An Intrinsic Relationship between Molecular Structure in Self-Assembled n-Alkylsiloxane Monolayers and Deposition Temperature. *J. Phys. Chem.* **1994**, *98*, 7877−7890.
(59) Kessel, C. R.; Granick, S. Formation and Characterizetion of a Highly Ordered and Well-Anchored Alkylsilane Monolayer on Mica by Self-Assembly. *Langmuir* **1991**, *7*, 532−538.
(60) Jeon, N. L.; Clem, P. G.; Nuzzo, R. G.; Payne, D. A. Patterning of Dielectric Oxide Thin Layers by Microcontact Printing of Self-Assembled Monolayers. *J. Mater. Res.* **1995**, *10*, 2996−2999.
(61) Jeon, N. L.; Hu, J. M.; Whitesides, G. M.; Erhardt, M. K.; Nuzzo, R. G. Fabrication of MOSFETs Using Soft Lithography. *Adv. Mater.* **1998**, *10*, 1466−1469.
(62) Xia, Y.; Whitesides, G. M. Soft Lithography. *Angew. Chem., Int. Ed. Engl.* **1998**, *37*, 551−575.
(63) Erhardt, M. K.; Nuzzo, R. G. Fabrication of Pt−Si Schottky Diodes Using Soft Lithographic Patterning and Selective Chemical Vapor Deposition. *Langmuir* **1999**, *15*, 2188−2193.
(64) Kim, E.; Xia, Y.; Whitesides, G. M. Polymer Microstructures Formed by Moulding in Capillaries. *Nature* **1995**, *376*, 581−584.
(65) Xia, Y.; Kim, E.; Whitesides, G. M. Micromolding of Polymers in Capillaries−Applications in Microfabrication. *Chem. Mater.* **1996**, *8*, 1558−1567.

AR960102N